Quadruple Metal−Metal Bonds with Strong Donor Ligands. Ultraviolet Photoelectron Spectroscopy of $M_2(form)_4$ (M = Cr, Mo, W; form = *N*,*N*′-diphenylformamidinate)

Dennis L. Lichtenberger,*,† Matthew A. Lynn,† and Malcolm H. Chisholm‡,§

Contribution from the Departments of Chemistry, The University of Arizona, Tucson, Arizona 85721, and Indiana University, Bloomington, Indiana 47405

Received August 23, 1999

Abstract: The He I photoelectron spectra of $M_2(form)_4$ (M = Cr, Mo, W; form = *N*,*N*′-diphenylformamidinate) and $Mo_2(cyform)_4$ (cyform = *N*,*N*′−dicyclohexylformamidinate) are presented. For comparison, the Ne I, He I, and He II photoelectron spectra of $Mo_2(p\text{-}CH_3\text{-}form)_4$ have also been obtained. The valence ionization features of these molecules are interpreted based on (1) the changes that occur with the metal and ligand substitutions, (2) the changes in photoelectron cross sections with excitation source, and (3) the changes from previously studied dimetal complexes. These photoelectron spectra are useful for revealing the effects that better electron donor ligands have on the valence electronic structure of $M_2(L^-L)_4$ systems. Comparison with the He I spectra of the isoelectronic $M_2(O_2CCH_3)_4$ compounds is particularly revealing. Unlike with the more electron-withdrawing acetate ligand, several formamidinate-based ionizations derived from the nitrogen p_π orbitals occur among the metal−metal σ, π, and δ ionization bands. Although these formamidinate-based levels are close in energy to the occupied metal−metal bonds, they have little direct mixing interaction with them. The shift of the metal−metal bond ionizations to lower ionization energies for the formamidinate systems is primarily a consequence of the lower electonegativity of the ligand and the better π donation into empty metal levels. The metal−metal δ orbital experiences some additional net bonding interaction with ligand orbitals of the same symmetry. Also, an additional bonding interaction from ligand-to-metal electron donation to the δ^* orbital is identified. These spectra suggest a greater degree of metal−ligand covalency than in the related $M_2(O_2CCH_3)_4$ systems. Fenske−Hall molecular orbital and density functional (ADF) calculations agree with the assignment and interpretation of these spectra. Calculated ionization energies are reported for $M_2(form)_4$ based on several different density functionals and with different orientations and substitutions for the phenyl rings. It is found that good estimates of the ionization energies are obtained when the truncated system $M_2(HN\text{-}(CH)NH)_4$, in which the phenyl groups are replaced by hydrogen atoms, is employed.

Introduction

Metal−metal interactions are central to the behavior of a wide variety of molecules, clusters, interfaces, and materials. An understanding of metal−metal interactions and their influence on chemistry is rooted in the electronic structure and bonding between just two metal atoms. As put forth by Cotton,[1] allotment of the dimetal-based valence electrons into molecular orbitals of σ, π, δ, δ^*, π^*, and σ^* symmetries provides a wealth of information regarding the reactivity and physical properties that a given dimetal system will possess. For instance, metal−metal and metal−ligand bond distances, diamagnetism and paramagnetism, electronic transitions and ionizations, redox activity, and the like are all relatively directly explained based on the simple metal−metal bonding manifold.[2] Detailed features of this bonding manifold have been most widely studied in molecules of the general formula M_2L_4, where the ligand set around the dimetal core approximates D_{4h} symmetry and each metal−metal orbital interaction is distinct by symmetry. Of primary concern to chemists is the effect that chemical tuning, including choice of metal and ligands, has on the reactivity and electronic properties of a system with metal−metal bonds.

The diphenylformamidinate ligand (commonly referred to as form = *N*,*N*′-diphenylformamidinate) has made possible the synthesis of dimetal compounds of more transition metals than any other ligand system. Currently, $M_2(form)_4$ compounds have been reported[3] for M = V, Cr, Mo, W, Re, Fe, Ru, Co, Rh, Ir, Ni, Pd, and Pt and $M_2(form)_2$ systems have been prepared[4] for M = Cu and Ag. Furthermore, due to the ease of preparation of this ligand system, substituents can easily be added to the phenyl ring to probe the long-range effect of electron-donating and -withdrawing substituents on the electronic structure of these compounds.[5−8] The stability and volatility of these compounds have rendered their study by photoelectron spectroscopy pos-

* To whom correspondence should be addressed.
† The University of Arizona.
‡ Indiana University.
§ Present address: Department of Chemistry, The Ohio State University, Columbus, OH 43210.

(1) Cotton, F. A. *Inorg. Chem.* **1965**, *4*, 334−336.
(2) Cotton, F. A.; Walton, R. A. *Multiple Bonds Between Metal Atoms*; Clarendon Press: Oxford, 1993.
(3) Cotton, F. A.; Haefner, S. C.; Sattelberger, A. P. *Inorg. Chem.* **1996**, *35*, 7350−7357.
(4) Cotton, F. A.; Feng, X.; Matusz, M.; Poli, R. *J. Am. Chem. Soc.* **1988**, *110*, 7077−7083.
(5) Lin, C.; Protasiewicz, J. D.; Smith, E. T.; Ren, T. *J. Chem. Soc. Chem. Commun.* **1995**, 2257−2258.
(6) Lin, C.; Protasiewicz, J. D.; Smith, E. T.; Ren, T. *Inorg. Chem.* **1996**, *35*, 6422−6428.
(7) Lin, C.; Protasiewicz, J. D.; Ren, T. *Inorg. Chem.* **1996**, *35*, 7455−7458.

10.1021/ja993065e CCC: $18.00
Published on Web 11/24/1999

sible, and photoelectron spectroscopy provides the most direct observation of the electronic structure features.

We present here the photoelectron spectra of the latest class of dimetal "paddlewheel" compounds: $M_2(form)_4$ (M = Cr, Mo, W). Assignment of the photoelectron spectra of the $M_2(form)_4$ compounds is greatly aided by the experimental and theoretical work that has been performed by numerous research groups on the tetracarboxylate compounds of dichromium, dimolybdenum, and ditungsten.[9−12] The structural similarity of the $M_2(O_2CCH_3)_4$ and $M_2(form)_4$ molecules is shown below, with the phenyl

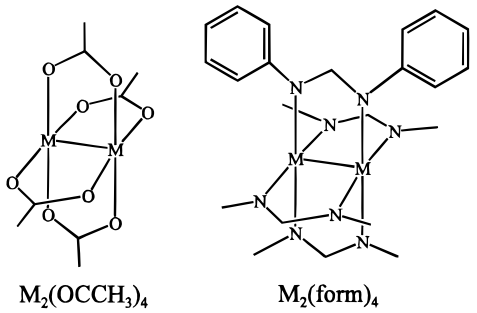

$M_2(OCCH_3)_4$ $M_2(form)_4$

groups of three of the diphenylformamidinate ligands removed for clarity. Understanding the valence electronic structure of the acetate systems assists spectral assignments for the formamidinates and gives insight into the ligand influences on the metal−metal bonding. In addition, we present the He I spectrum of $M_2(cyform)_4$ (cyform = *N*,*N*′-dicyclohexylformamidinate) to help identify a ligand-based ionization that is obscured in the spectra of the phenyl ring-containing systems. This work serves as the foundation for understanding the photoelectron spectra of other $M_2(form)_4$ (M = Ru, Rh, Pd) systems as well as of variously functionalized $Mo_2(form)_4$ compounds that are currently being investigated.[13,14]

Experimental Section

Photoelectron Spectra. Samples were prepared according to published procedures.[15,16] The photoelectron spectra were collected on a spectrometer equipped with specially designed photon sources, ionization cells, 36 cm radius hemispherical analyzer (McPherson), power supplies, counter interface, and collection methods that have been described elsewhere.[17−19] The spectra were measured with a stainless steel sample ionization cell at 230−300 °C, depending on the particular compound being studied. Specific sublimation temperatures for these systems are as follows: $Cr_2(form)_4$ (290 °C), $Mo_2(form)_4$ (225 °C), $Mo_2(p\text{-}CH_3\text{-}form)_4$ (260 °C), $Mo_2(cyform)_4$ (230 °C), and $W_2(form)_4$ (245 °C). The argon ionization at 15.759 eV was used as an internal calibration lock of the energy scale. Instrument resolution was better than or equal to 0.030 eV, as measured by the full-width at half-maximum of the Ar $^2P_{3/2}$ ionization, during all experiments.

In the figures of the data, the vertical length of each point represents the experimental variance of that point. The ionization bands are represented analytically with the best fit (program FP[20]) of asymmetric Gaussian peaks.[21] These peaks are defined with position, amplitude, half-width for high ionization energy side, and half-width for the low ionization energy side of the peak. The reproducibility of the peak positions and widths is typically ±0.02 eV (3σ) when ionization bands are not substantially overlapping. The number of peaks used in a fit is based on the visible features of a given band profile and the minimum number of peaks necessary to give the best statistical fit.[21] The parameters describing an individual ionization peak are less certain when two or more peaks are close in energy and overlap. The confidence limits for the relative integrated band areas are about 5%, with the primary source of uncertainty being the determination of the baseline subtracted from the peak. For representation of He II data, the position and width values of the asymmetric Gaussians were all constrained to the He I values because the better signal-to-noise ratio of the He I spectra allows these values to be determined more accurately. The amplitudes were then allowed to vary to account for the different photoionization cross sections for He II. Fitting procedures are described in more detail elsewhere.[21] The peak positions and relative peak areas for the low-energy bands in the He I spectra of $M_2(form)_4$ (M = Cr, Mo, W) and $Mo_2(cyform)_4$ are given in Table 1. The same parameters are provided in Table 2 for the Ne I, He I, and He II photoelectron spectra of $Mo_2(p\text{-}CH_3\text{-}form)_4$.

Table 1. Peak Positions, Average Full-Widths at Half Maximum, Relative Peak Areas, and Peak Assignments for Low-Energy He I Ionizations of $M_2(form)_4$ (M = Cr, Mo, W) and $Mo_2(cyform)_4$

compd	position (eV)	half-width (eV)	rele area	label[a]
$Cr_2(form)_4$	6.44	0.37	1	δ
	6.66	0.21	1.0	a_{1u}
	6.87	0.26	2.1	e_g
	7.08	0.29	1.3	$\sigma + \pi$
$Mo_2(form)_4$	5.63	0.32	1	δ
	6.45	0.29	1.3	a_{1u}
	6.80	0.39	2.6	e_g
	7.32	0.56	2.7	$\sigma + \pi$
	7.88	0.31	1.8	b_{1u}
$Mo_2(cyform)_4$	5.33	0.33	1	δ
	6.51	0.24	1.3	a_{1u}
	6.84	0.35	2.2	e_g
	7.19	0.32	1.8	π
	7.43	0.28	1.0	σ
	7.76	0.52	2.8	b_{1u}
$W_2(form)_4$	5.23	0.21	1	δ
	6.58	0.32	1.8	a_{1u}
	6.91	0.42	3.0	e_g
	7.33	0.38	2.0	π
	7.54	0.24	1.2	σ
	7.91	0.33	1.9	b_{1u}

[a] Group theoretical labels denote ligand-based orbitals and the traditional Greek characters denote the predominantly metal−metal bonding and antibonding MOs.

Calculations. A molecular orbital calculation was performed on the $Mo_2(form)_4$ system via the Fenske−Hall method[22] for comparison not only with previous calculations on M−M bonded systems but also with the results of the density functional work presented here. Atomic basis functions were generated using the method of Bursten et al.[23] Contracted double-ζ functions were used for the Cr, Mo, and W valence d atomic orbitals (AOs) and for the carbon and nitrogen 2p atomic orbitals. Basis

(8) Lin, C.; Ren, T.; Valente, E. J.; Zubkowski, J. D.; Smith, E. T. *Chem. Lett.* **1997**, 753−754.
(9) Coleman, A. W.; Green, J. C.; Hayes, A. J.; Seddon, E. A.; Lloyd, D. R.; Niwa, Y. *J. Chem. Soc. Dalton Trans.* **1979**, 1057−1064.
(10) Lichtenberger, D. L.; Blevins, C. H. *J. Am. Chem. Soc.* **1984**, *106*, 1636−1641.
(11) Lichtenberger, D. L.; Ray. C. D.; Stepniak, F.; Chen, Y.; Weaver, J. H. *J. Am. Chem. Soc.* **1992**, *114*, 10492−10497.
(12) Lichtenberger, D. L.; Johnston, R. L. In *Metal−Metal Bonds and Clusters in Chemistry and Catalysis*; Fackler, J. P., Ed.: Plenum: New York, 1989; pp 1−24.
(13) Lichtenberger, D. L.; Lynn, M. A.; Chisholm, M. H. 217th National Meeting of the American Chemical Society, Anaheim, CA, April 1999; American Chemical Society: Washington, DC., 1999; Abstract 027-INOR.
(14) Lichtenberger, D. L.; Lynn, M. A.; Chisholm, M. H. 217th National Meeting of the American Chemical Society, Anaheim, CA, April 1999; American Chemical Society: Washington, DC., 1999; Abstract 253-INOR.
(15) Cotton, F. A.; Feng, X.; Matusz, M. *Inorg. Chem.* **1989**, *28*, 594−601.
(16) Cotton, F. A.; Ren, T. *J. Am. Chem. Soc.* **1992**, *114*, 2237−2242.
(17) Lichtenberger, D. L.; Kellogg, G. E.; Kristofzski, J. G.; Page, D.; Turner, S.; Klinger, G.; Lorenzen, J. *Rev. Sci. Instrum.* **1986**, *57*, 2366.
(18) Jatcko, M. E. *Diss. Abstr. Int. B* **1990**, *51*, 200.
(19) Renshaw, S. K. *Diss. Abstr. Int. B* **1992**, *51*, 5259.
(20) Chandramouli, G. V. R.; Subramanian, L.; Manoharan, P. T. *Comput. Chem.* **1990**, *14*, 257.
(21) Lichtenberger, D. L.; Copenhaver, A. S. *J. Elect. Spec. Relat. Phenom.* **1990**, *50*, 335−352.
(22) Fenske, R. F.; Hall, M. B. *Inorg. Chem.* **1972**, *11*, 768−775.
(23) Bursten, B. E.; Jensen, J. R.; Fenske, R. F. *J. Chem. Phys.* **1978**, *68*, 3320−3321.

Table 2. Peak Positions and Relative Areas in the Ne I, He I, and He II Photoelectron Spectra of $Mo_2(p\text{-}CH_3\text{-form})_4$

	rel peak areas			
position (eV)	Ne I	He I	He II	label
5.60	1	1	1	Mo−Mo δ
6.37	3.02	1.36	1.41	ligand-based a_{1u}
6.71	5.46	2.88	2.82	ligand-based e_g
7.27	*a*	*a*	*a*	Mo−Mo $\sigma + \pi$
7.6	*a*	*a*	*a*	ligand-based b_{1u}

[a] Unable to determine due to overlap with tail of intense ionization band and uncertainty in the baseline.

functions for the metal atoms were derived for the 1+ oxidation state. Ground-state atomic configurations were used for the basis functions of all other atoms. The bond distances and angles were taken from the reported crystal structures[15,16] and the total geometry of the system was idealized to D_{4h} symmetry. To achieve the symmetry of this point group, the N−Mo−Mo−N torsion angle, which is 3.2° in the published crystal structure, was set to 0°. The orientations of the phenyl rings with respect to the N−C−N plane are not all the same in the crystal structures. This matter will be a point of discussion for the calculation of ionization energies of the molecules in the gas phase.

Density functional calculations were performed with the ADF (Amsterdam Density Functional) package, Version 2.3.0.[24−26] Results from LDA (Xα) and GGA (BLYP) computations are presented here. For the full systems (i.e., including the phenyl rings), basis sets used for the transition metal atoms were from set IV (triple-ζ Slater-type orbitals) and for C, N, and H were from set II (double-ζ STOs). For Mo ($n = 3$) and W ($n = 4$), the core orbitals were defined as the *n*d orbitals and lower. For Cr, the 2p orbitals and lower were considered core. Single-point calculations with triple-ζ functions on all of the atoms were performed for the neutral molecules and a similar ordering of valence orbitals (i.e., ligand orbitals less stable than metal-based orbitals) was obtained. For the model systems ($M_2(HNCHNH)_4$), all basis sets were from set IV. Ionization energies for the full molecules and for the truncated systems ($M_2(HN(CH)NH)_4$), using D_{4h} symmetry, were calculated by determining the total energy difference between the neutral and cationic systems, with electrons being removed from the various valence molecular orbitals. The default SCF convergence criterion was employed.

Background

Preliminary Considerations. The present study relates directly to previous photoelectron investigations of metal−metal bonded systems, and the information from these earlier studies is important to the foundation of the present work. The metal−metal bonding manifold is a classic textbook subject and will only be reviewed briefly here. The Cr, Mo, and W atoms in the $M_2(form)_4$ molecules are formally in the +II oxidation state with d^4 configurations. According to the M−M bonding interactions these d electrons occupy orbitals of σ, π, and δ symmetry, each of which has separate symmetry properties under the D_{4h} point group. Therefore, ionization of an electron from each of these bonds may give rise to a separate feature in a photoelectron spectrum because mixing of the various bonding components of the metal−metal bond is forbidden by symmetry in the absence of spin−orbit coupling and configuration interaction.

(a) The $M_2(O_2CR)_4$ Compounds: Points of Primary Reference. A conclusive assignment of these ionizations in the gas-phase photoelectron spectra of these systems has only been realized relatively recently.[12] The gas-phase and thin-film He I photoelectron spectra of $M_2(O_2CCH_3)_4$ (M = Cr, Mo, W) have been published previously by our group.[27] In general, assignment of the M−M π and δ features (M = Mo, W) as the two bands of lowest ionization energy in these spectra is accepted. However, understanding the strength of the M−M σ bond and assigning its ionization feature have been a considerable challenge. Scattered wave DV-Xα calculations originally suggested that the ionization feature resulting from the M−M σ bond, which was believed to be the strongest of the metal−metal electronic interactions because of the direct overlap between the valence d_z^2 atomic orbitals on each metal center, should lie several electronvolts higher than the π bond in ionization energy.[28−30] Some studies therefore assigned peaks higher than ca. 10 eV as arising from the ionization of an electron from the M−M σ bond. As for the analogous chromium system, the photoelectron spectrum exhibits a single, broad ionization feature, which is generally thought to arise from the removal of electrons from the Cr−Cr σ, π, and δ bonds. However, the $\sigma^2\pi^4\delta^2$ configuration may only represent a small percentage of the complete ground-state wave function.[31] In other words, the electronic interactions in Cr−Cr quadruple bond-containing systems may instead arise from antiferromagnetism, superexchange, or a combination of these two effects. Hence, assignment of various features of the broad band as resulting from removal of electrons from the σ, π, and δ bonds may not be appropriate.

(b) Assignment of $M_2(O_2CR)_4$ Metal-Based Ionizations. Despite the early computational studies that led to the prediction that the M−M valence σ orbital should have considerably greater bonding character than the π and δ orbitals, thin-film surface ultraviolet photoelectron spectroscopy (UPS) experiments from our laboratory showed that electronic occupation of the M−M π orbitals gives the greatest bonding character and that the σ ionization is in the same energy region as the π ionization.[27] In the case of the gas-phase photoelectron spectroscopy study of $Mo_2(O_2CCH_3)_4$, the σ and π ionizations are believed to be energetically coincident while the removal of an electron from the δ bond lies ca. 1.70 eV lower in energy. A shoulder, not observed in the gas-phase spectrum, is found on the low ionization energy side of the Mo−Mo π band in the surface photoelectron spectrum. It is thought that this feature occurs in the thin-film surface spectrum of $Mo_2(O_2CCH_3)_4$ because the Mo−Mo σ bond is destabilized in the solid phase as a result of its filled−filled interaction with an oxygen atom lone pair from an adjacent $Mo_2(O_2CR)_4$ molecule.

For the $W_2(O_2CR)_4$ systems in the gas phase, the σ ionization appears as a separate, sharp feature on the high ionization energy side of the W−W π ionization, which is separated from the δ band by 1.70−1.80 eV.[12,32] The photoelectron spectrum of a thin film of $W_2(O_2CCH_3)_4$ shows only two features below 11 eV and the band assigned to the π ionization increases in intensity relative to the δ band.[27] This spectral change occurs as a result of the destabilization of the W−W σ bond, which is then energetically coincident with the W−W π band in the solid phase.

(c) $M_2R'_2(O_2CR)_4$ Compounds. Additional support for these assignments of the Mo−Mo and W−W σ ionizations is found in the photoelectron spectra of $M_2(np)_2(O_2CCH_3)_4$ (M = Mo, W; np = neopentyl).[33] Comparison of the spectra of $Mo_2(O_2CCH_3)_4$ and $Mo_2(np)_2(O_2CCH_3)_4$ shows that an additional ionization band is present between the π and δ bands for the neopentyl system. For the W_2 systems, the sharp σ ionization feature of $W_2(O_2CCH_3)_4$ is not present in the spectrum of $W_2(np)_2(O_2CCH_3)_4$ and the W−W π band is more broad for the neopentyl system. These results suggest that the M−M σ bond has been oxidized upon the attachment of the two alkyl substituents to the metal centers and the formation of M−C σ bonds. The additional ionization observed for $Mo_2(np)_2(O_2CCH_3)_4$ and the broadening of the π band of $W_2(np)_2(O_2CCH_3)_4$ are thus indicative of ionizations from the M−C σ bonds.

$M_2(O_2CH)_4$ and $Mo_2(HNCHNH)_4$. General Theory. To understand the interactions of the ligand-based orbitals with those of the dimetal

(24) ADF 2.3.0, Theoretical Chemistry, Vrije Universiteit, Amsterdam.
(25) te Velde, G.; Baerends, E. J. *J. Comput. Phys.* **1992**, *99*, 84−98.
(26) Baerends, E. J.; Ellis, D. E.; Ros, P. *Chem. Phys.* **1973**, *2*, 41−51.
(27) Lichtenberger, D. L.; Kristofzski, J. G. *J. Am. Chem. Soc.* **1987**, *109*, 3458−3459.
(28) Norman, J. G.; Kolari, H. J. *J. Am. Chem. Soc.* **1975**, *97*, 33−37.
(29) Norman, J. G.; Kolari, H. J. *J. Chem. Soc., Chem. Commun.* **1975**, 649−651.
(30) Norman, J. G.; Kolari, H. J.; Gray, H. B.; Trogler, W. C. *Inorg. Chem.* **1977**, *16*, 987−993.
(31) Hall, M. B. *Polyhedron* **1987**, *6*, 679−684.
(32) Bancroft, G. M.; Pellach, E.; Sattelberger, A. P.; McLaughlin, K. W. *J. Chem. Soc., Chem. Commun.* **1982**, 752−754.
(33) Chisholm, M. H.; Clark, D. L.; Huffman, J. C.; Van der Sluys, W. G.; Kober, E. M.; Lichtenberger, D. L.; Bursten, B. E. *J. Am. Chem. Soc.* **1987**, *109*, 6796−6816.

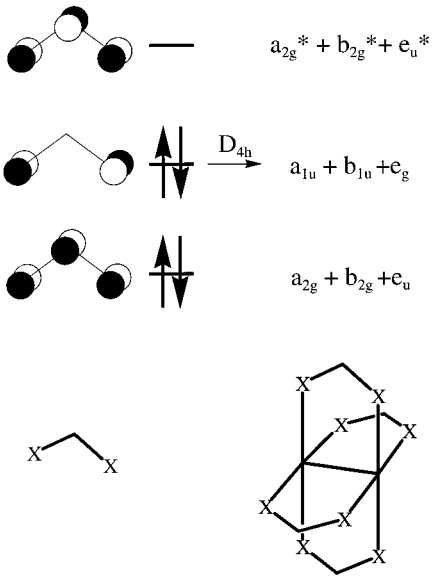

Figure 1. The three π symmetry combinations possible for X−C−X.

fragment, it is helpful to compare the pertinent bonding modes of the carboxylate and formamidinate systems. The electronic structure of the acetate ligand is easily understood by partitioning the total number of valence electrons into the σ and π bonds that the simplest carboxylate, O−C(H)−O$^-$, possesses. This moiety has 18 valence electrons, 6 of which are involved in O−C and H−C σ bonding. Four electrons are located in two oxygen lone pairs that are used to form σ bonds with the metal centers. Another four electrons are found in two additional lone pairs, one pair on each oxygen atom, and are analogous to the in-plane oxygen lone pair in water. The remaining four electrons are in the π network of the carboxylate ligand. The three π combinations, composed of the two O and one C $2p_\perp$ atomic orbitals, are shown in Figure 1. Note that the lowest of these three is O−C π bonding, the highest is O−C π antibonding, and the middle nonbonding combination is located entirely on the O atoms. The four electrons available for the π network occupy the two combinations of lowest energy.

The simplest formamidinate, HN−C(H)−NH$^-$, also has 18 valence electrons, 6 of which are involved in σ bonds (C−H and two N−C bonds), 4 are used by the nitrogen atoms to form σ bonds with the metal centers, and 4 are in the same type of π combinations found for the carboxylate systems. The four electrons of the carboxylate that were in the in-plane oxygen lone pair orbitals directed away from the metal atoms are now in the N−H σ bonds of the formamidinate.

When four of the carboxylate or formamidinate ligands are located around two metal centers to form an $M_2(X-C(R)-X)_4$ system with D_{4h} symmetry, each X−C−X orbital forms four linear combinations. For this discussion, group theoretical labels will be used to denote ligand-based orbitals and the traditional Greek characters will be employed to describe the metal−metal bonding and antibonding MOs. Of course, these metal−metal interactions can also be described by group theoretical labels, which will be emphasized where appropriate.

The out-of-phase electron pair orbitals which lie in the X−C−X plane and are primarily directed toward the exterior of the molecule also include some X−C−X σ bonding character. These orbitals form linear combinations of symmetries a_{2u}, b_{2u}, and e_g for the four ligands in D_{4h} symmetry. One of the four combinations of the in-plane electron pairs for a carboxylate and formamidinate system is compared in Figure 2. For the carboxylate these are primarily a combination of the in−plane oxygen lone pairs while for the formamidinate these are a combination of the N−H bonds. The similarity is evident. By symmetry only the e_g set can interact in a bonding fashion with the M−M π^* antibond; the rest are strictly ligand based. With the presence of the additional substituent on the N atom of a formamidinate ligand (an H atom in the figure, but a phenyl group in the systems actually examined experimentally), these orbitals that are lone pairs for the O-donor ligands become N−H (or N−C_{phenyl}) σ bonding in nature and are moved to

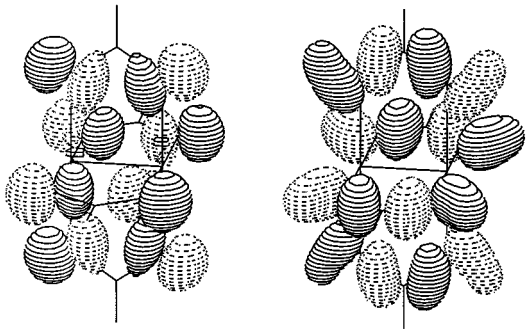

Figure 2. The a_{1u} combination of the in-plane O lone pairs and N−H bonds as determined via the Fenske−Hall method.

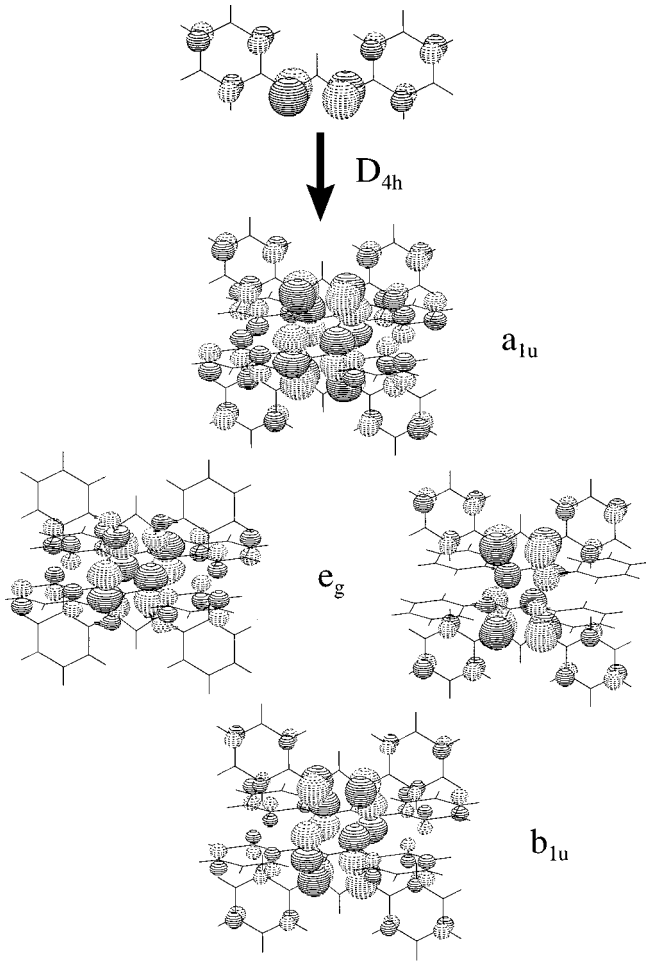

Figure 3. The a_{1u}, e_g, and b_{1u} combinations of the HOMO of the carboxylate and formamidinate ligands under D_{4h} symmetry.

higher ionization energy by ca. 3 eV in the formamidinate systems relative to the carboxylates.

The lowest of the X−C−X π bonding orbitals in Figure 1 forms linear combinations with symmetries a_{2g}, b_{2g}, and e_u when the four ligands are arranged in the D_{4h} geometry. The b_{2g} combination has the appropriate symmetry and spatial orientation to interact with the M−M δ bond and can influence this ionization.

The middle π orbital forms combinations of a_{1u}, b_{1u}, and e_g symmetry, which are shown in Figure 3. Of these last three combinations, only the b_{1u} arrangement has the proper symmetry features to interact with a metal-based fragment orbital, namely the δ^*. This interaction provides an additional mechanism for bonding and electron donation to the metal center. The ligand e_g orbitals, although of the same symmetry as the M−M π^* antibond, are in a plane orthogonal to these metal orbitals

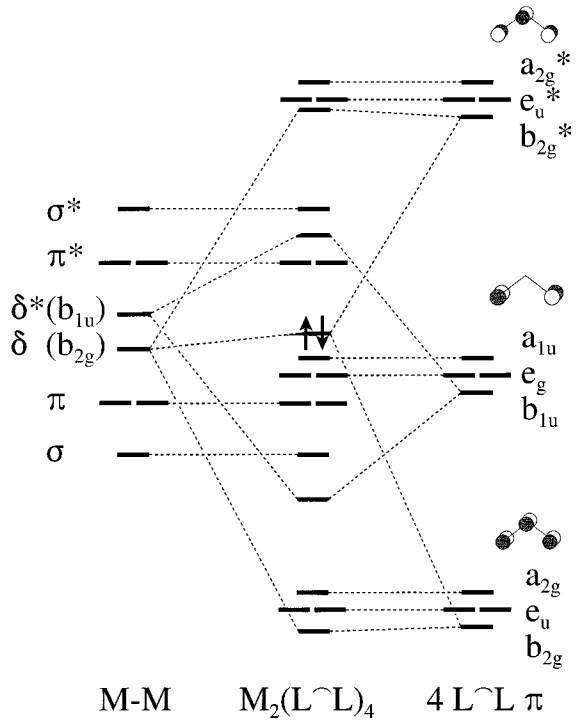

Figure 4. Molecular orbital diagram depicting π-type ligand interactions with the metal−metal bonding and antibonding orbitals. The arrows represent the HOMO of a system that contains a metal−metal quadruple bond.

and cannot mix. As will be seen, the a_{1u} and e_g combinations are entirely ligand based and are found at lower ionization energy than the metal−ligand bonding b_{1u} orbital. The a_{1u} set is expected to be found at a slightly lower ionization energy than the e_g combination because the former has electron density on all four ligands with an antibonding interaction between the $p_\perp$ AOs on adjacent ligands while the latter only has electron density on two ligands located opposite each other.

The antibonding X−C−X π bonding orbital, like the X−C−X π bonding orbital, forms linear combinations with symmetries a_{2g}, b_{2g}, and e_u when the four ligands are arranged under D_{4h} symmetry. For this discussion, an asterisk will be added to these last three combinations (i.e., a_{2g}*, b_{2g}*, and e_u*) to denote the X−C π* antibonding character that these fragment orbitals possess. Because of its symmetry, the b_{2g}* combination can also interact with the M−M δ bond.

A qualitative MO diagram that summarizes these interactions is presented in Figure 4. The metal−metal bonding and antibonding orbitals, arranged in their typical textbook ordering, are presented on the left side of this figure. The combinations of all of the ligand π-type orbitals are shown on the right side of the diagram. The strongest metal−ligand interaction in this region, because of the good overlap and energy match between the fragment orbitals, is between the M−M δ* antibond and ligand b_{1u} orbital. Based on ionizations and calculations to be discussed, the metal−ligand bonding combination is stabilized below the M−M σ bond and the corresponding metal−ligand antibonding combination (the orbital usually called the M−M δ* antibond) is destabilized above the M−M π* orbital. The second metal−ligand interaction in this region, between the M−M δ bond and the ligand b_{2g} and b_{2g}* combinations, is much weaker. Although the metal−ligand overlap is similar to that observed for the b_{1u} combinations, the energy match between the δ bond and these combinations is worse. The $\delta-b_{2g}$ interaction in this region is antibonding while for $\delta-b_{2g}$* the interaction is bonding. The result is that depending on the relative amounts of b_{2g} and b_{2g}* character in this molecular orbital, the M−M δ ionization can be slightly stabilized or destabilized. The remainder of orbitals in this diagram are essentially nonbonding and are either metal or ligand based.

Considering the difference in atomic composition between the acetate and phenylformamidinate ligand systems, the nonbonding (middle orbital in Figure 1) $p_\perp$ combination is expected to be localized entirely on the O atoms for the O−C−O unit. However, because of the phenyl rings bound to the N atoms in the formamidinates, these four $p_\perp$ combinations may be conjugated to the phenyl π systems depending on the orientation of the phenyl rings. On the basis of the relative electronegativities of N and O it is expected that ionizing an electron from these orbitals should require less energy for the tetraformamidinates than for the tetracarboxylates.

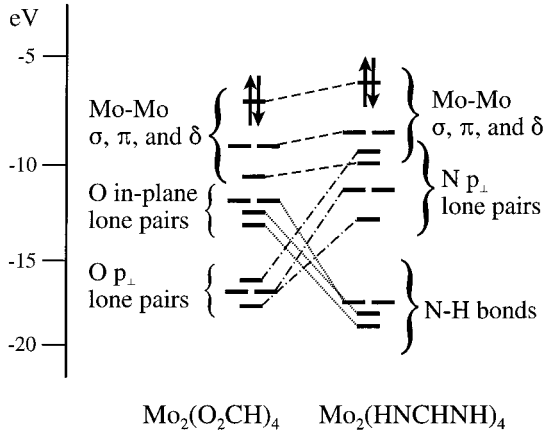

Figure 5. Correlation diagram between analogous molecular orbitals of $Mo_2(O_2CH)_4$ and $Mo_2(HNC(H)NH)_4$. The arrows represent the HOMO.

Table 3. Fenske−Hall Calculated Relative Energies and Orbital Compositions for the Valence Orbitals of $Mo_2(form)_4$[a]

calcd energy (eV)	orbital description	orbital composition
−8.25	Mo−Mo δ bond	84% Mo 15% C (N−**C**−N)
−9.70	ligand-based a_{1u}	53% N 42% C (aryl)
−10.32	ligand-based e_g	51% N 44% C (aryl)
−10.69	Mo−Mo π bond	90% Mo 7% N
−11.68	Mo−Mo σ bond	91% Mo 8% N
−11.92	ligand-based b_{1u}	13% Mo−Mo δ* 30% N 57% C (aryl)

[a] The phenyl rings are coplanar with the ligand.

Figure 5 presents a summary of the relative energies, as obtained by the Fenske−Hall method, of the ligand- and metal-based valence molecular orbitals. For the tetracarboxylates, the in- and out-of-plane O-based lone pair combinations are all found at higher ionization energies than are the metal−metal bonding orbitals. The combinations that are the O-based in-plane lone pairs in the acetates are more tightly bound in the formamidinates because they possess N−C_{phenyl} σ bonding character. For the tetraformamidinates, the $p_\perp$ combinations move to lower ionization energy than those of the tetracarboxylates mostly because of the difference in electronegativity between N and O. In fact, the Fenske−Hall method predicts that for the HN(CH)NH ligand system, at least one of these combinations is found energetically between the Mo−Mo σ and π orbitals, and as will be seen in the spectra of the tetraphenylformamidinates, ionizations from several of these orbitals actually occur in the same energy region as those from the metal−metal bonds.

A Fenske−Hall calculation on the D_{4h} $Mo_2(form)_4$ system with the full diphenylformamidiniate ligand predicts a ground-state molecular orbital ordering of the eight highest valence molecular orbitals as shown in Table 3. The highest occupied molecular orbital (HOMO) of this system is calculated to be the Mo−Mo δ bond, which contains approximately 15% ligand character. This orbital is followed by the a_{1u} and e_g ligand-based orbitals. Next are the Mo−Mo π and σ bonds, which are about 90% metal in character. These orbitals are followed

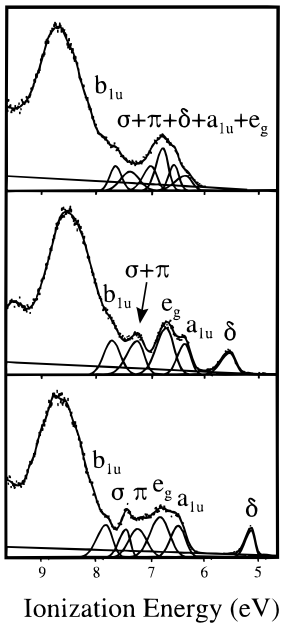

Figure 6. He I photoelectron spectra of $M_2(form)_4$ (M = Cr (top), Mo (middle), W (bottom)).

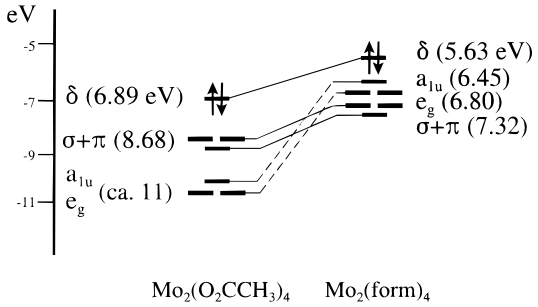

Figure 7. Correlation diagram of the valence ionization energies of $Mo_2(O_2CCH_3)_4$ and $Mo_2(form)_4$. The arrows represent the HOMO.

by the fourth (b_{1u}) ligand $p_\perp$-based combination, which contains ca. 13% metal−metal δ^* character. Higher still in ionization energy are the occupied π orbitals of the phenyl rings and the deeper intraligand σ and π bonding orbitals.

Results and Discussion

Information from Ionization Characteristics. The He I valence photoelectron spectra of $M_2(form)_4$ (M = Cr, Mo, W) are presented in Figure 6. All spectra have a broad intense ionization band spanning from 8 to 9.5 eV, characteristic of phenyl π ionizations. The spectrum of $Mo_2(form)_4$ shows the best separation of the low-energy ionizations. In this spectrum, a single ionization band appears at 5.63 eV followed by features at 6.45, 6.80, and 7.32 eV. A single ionization feature appears at 5.23 eV for $W_2(form)_4$ followed by overlapping ionizations from 6.5 to 8 eV. The spectrum of $W_2(form)_4$ exhibits a sharp feature at 7.54 eV as well as a broadening near 7.32 eV that is not evident in the spectra of the Cr_2 and Mo_2 systems. In the spectrum of $Cr_2(form)_4$, the features in the region 6.25−8.25 are much more broad than those for the Mo_2 and W_2 systems.

Assignment of Spectral Features: The Mo- and W-Based σ, π, and δ and Ligand-Based a_{1u} and e_g Ionizations. The correlation of ionization energies and assignments of the spectra of $M_2(O_2CCH_3)_4$ and $M_2(form)_4$ (M = Mo, W) is illustrated in Figures 7 and 8. Comparison of the behavior of the first ionization band for the Mo_2 and W_2 systems with those previously observed for the $M_2(O_2CCH_3)_4$ systems indicates that

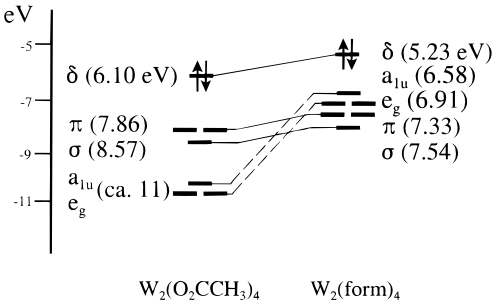

Figure 8. Correlation diagram of the valence ionization energies of $W_2(O_2CCH_3)_4$ and $W_2(form)_4$. The arrows represent the HOMO.

Table 4. Energies of the M−M δ, Ligand b_{2g}, and Ligand b_{2g}* Fragment Orbitals and Their Percent Contributions to the M−M δ Bonding Molecular Orbital as Determined by the Fenske−Hall Method

	fragment energies (eV)			M−M δ orbital composition (%)		
	M−M δ	b_{2g}	b_{2g}*	M−M δ	b_{2g}	b_{2g}*
$Mo_2(O_2CCH_3)_4$	−8.5	−18.3	2.8	87.9	7.5	4.5
$Mo_2(HN(CH)NH)_4$	−7.6	−17.6	4.1	86.1	5.3	8.6
$W_2(O_2CCH_3)_4$	−7.3	−18.6	2.5	84.7	7.0	8.2
$W_2(HN(CH)NH)_4$	−6.4	−17.4	2.7	78.3	5.5	16.2

these features correspond to ionization of an electron from the M−M δ bond. The shift of these ionizations to lower energies for the $M_2(form)_4$ species is indicative of the more electron-donating nature of the formamidinate ligand versus the acetate: 1.25 eV for M = Mo and 0.87 eV for M = W. These shifts are dependent on the amounts of the metal δ and ligand b_{2g} and b_{2g}* fragment character that contribute to the M−M δ bonding molecular orbital. Energies of these fragment orbitals and their relative contributions as determined from Fenske−Hall calculations on the $M_2(O_2CCH_3)_4$ and $M_2(HN(CH)NH)_4$ (M = Mo, W) systems are presented in Table 4. The M−M δ fragment orbitals of all of the systems have similar energy matches (ca. 10 eV) with the b_{2g} and b_{2g}* fragment orbitals. The amount of ligand b_{2g} character is also similar (5.3−7.5%) for all of these molecules. However, the amount of ligand b_{2g}* character varies considerably among the systems and is larger for the formamidinates than for the acetates. Remembering that the δ−b_{2g}* interaction is bonding, the stabilizing effect on the W−W δ ionization in $W_2(HN(CH)NH)_4$ is the greatest of all of the systems. The smaller shift of the M−M δ ionization band from the acetate to the formamidinate for M = W is therefore consistent with the larger amount of ligand b_{2g}* character contained in this molecular orbital. Because there is less ligand b_{2g}* character in the Mo−Mo δ bonding molecular orbital for $Mo_2(HN(CH)NH)_4$, the δ ionization for this system is not stabilized as much as for the tungsten analogue, and the shift of the δ ionization is larger between $Mo_2(O_2CCH_3)_4$ and $Mo_2(form)_4$ than for the analogous tungsten systems.

The shift of the δ ionization upon changing the metal from Mo to W is less for the tetraformamidinate series (0.40 eV) than for the analogous tetraacetates (0.80 eV). This also follows from the greater b_{2g}* character in the M−M δ bonding molecular orbital of the tetraformamidinate molecules. In general, for molecular systems that possess the same ligand set but different metal centers, the difference in energy between an analogous orbital in each system will be smaller for the orbital with less metal and more ligand character. Thus, there is more ligand character in the δ ionization of the tetraformamidinate series than in the tetraacetates.

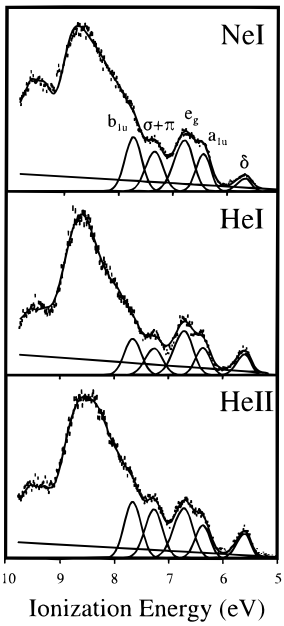

Figure 9. Ne I, He I, and He II photoelectron spectra of Mo_2(*p*-CH_3-form)$_4$.

The spectra of the tetraacetates also aid in the assignment of the σ and π ionizations for Mo_2(form)$_4$ and W_2(form)$_4$,. The single band assigned to the ionization from the σ and π bonds of $Mo_2(O_2CCH_3)_4$ occurs at 8.68 eV, the sharp σ ionization of $W_2(O_2CCH_3)_4$ appears at nearly the same energy (8.57 eV), and the π ionization of $W_2(O_2CCH_3)_4$ occurs at 7.86 eV. The sharp ionization at 7.54 eV in the spectrum of W_2(form)$_4$ occurs at an energy similar to that of the more broad peak at 7.32 eV for Mo_2(form)$_4$, suggesting that the former is due to the W−W σ bond and the latter from the Mo−Mo σ and π bonds. The energy gap between the δ and σ/π bands for Mo_2(form)$_4$ is therefore the same as for $Mo_2(O_2CCH_3)_4$: 1.70 eV. Additional ionization intensity near 7.3 eV occurs for the W system. Considering the separation of the σ and π bands in the gas-phase photoelectron spectrum of $W_2(O_2CCH_3)_4$ and the absence of this feature in the Mo_2(form)$_4$ spectrum, the ionization intensity in this region must be from the W−W π bond. The energy separation between this peak and the W−W σ ionization is ca. 0.30 eV, which is smaller than that found for the tetraacetate (0.71 eV) but is comparable to that found for $W_2Cl_4(P(CH_3)_3)_4$ (0.40 eV).[34] Because of the considerable overlap of the W−W σ and π ionization bands with the ligand-based a_{1u} and e_g features, it is difficult to determine the exact energy difference between the σ and π ionizations.

The remaining features to be addressed are those that arise from the ligand-based a_{1u}, e_g, and b_{1u} valence orbitals. The ratio of the areas of the peaks in the Mo_2(form)$_4$ spectrum at 6.45 and 6.80 eV is near 1:2, suggesting that the former ionization is from a singly degenerate orbital and the latter is from a set of doubly degenerate orbitals. Such an assumption can only rigorously be made if the orbital compositions of the MOs that give rise to the two ionizations are identical. Fenske−Hall calculations predict that the electron density of the a_{1u} and e_g orbitals is entirely based on the ligands (i.e., no metal character is possible by symmetry). Therefore, the assignment of these peaks as arising from ionizations from the ligand-based a_{1u} and e_g orbitals is appropriate. As for the metal−ligand bonding b_{1u} ionization, at this point in the discussion only a tentative assignment can be made. It is possible that the shoulder on the low ionization energy side of the phenyl ring ionizations can be attributed to the ionization from this b_{1u} orbital. The Fenske−Hall calculation for Mo_2(form)$_4$ suggests that the next highest MO in ionization energy to the Mo−Mo σ and π bonds is the b_{1u} orbital. This placement is reasonable considering the proximity of the band to the other two ionization bands attributed to the similar a_{1u} and e_g ligand-based MOs as well as to the metal−ligand bonding nature of the b_{1u} orbital. A more conclusive argument for this assignment, however, can only be made by employing a formamidinate ligand that does not contain unsaturated substituents. This matter will be examined shortly.

(34) Cotton, F. A.; Hubbard, J. L.; Lichtenberger, D. L.; Shim. I. *J. Am. Chem. Soc.* **1982**, *104*, 679−686.

Table 5. Valence Ionization Energies (in eV) Calculated with the ADF Package for Mo_2(form)$_4$ and Mo_2(HN(CH)NH)$_4$ Using the Xα Method[a]

	Mo_2(form)$_4$				
ionization	D_{4h}; 0°	D_4; 45°	D_{4h}; 90°	Mo_2(HN(CH)NH)$_4$	Mo_2(form) (exptl)
Mo−Mo δ bond	6.04	5.87	5.77	5.31	5.63
ligand-based a_{1u}	5.23	5.41	5.66	5.41	6.45
ligand-based e_g	5.54	5.67	6.06	5.93	6.80
Mo−Mo π bond	6.87	6.74	6.42	7.08	7.32
Mo−Mo σ bond	7.72	6.85	6.54	7.14	
ligand-based b_{1u}	6.32	6.44	7.25	7.28	7.88

[a] Angles refer to the rotation of the phenyl rings out of the N−C−N plane. Double-ζ functions have been used on all nonmetal atoms.

The Ne I, He I, and He II spectra of Mo_2(*p*-CH_3-form)$_4$ are shown in Figure 9. This figure demonstrates the inability of He I/He II comparisons to confirm assignments for these systems. From Table 2 it is evident that the areas of the metal-based δ and the ligand-based a_{1u} and e_g ionization bands do not change relative to each other. This observation is in agreement with calculated photoionization cross sections,[35] which predict that in a He II photoelectron spectrum, the areas of nitrogen- and carbon-based ionization bands should drop in intensity by 55% and 69%, respectively, relative to their areas in a He I spectrum. However, the areas of Mo- and W-based bands are expected to fall by essentially the same amount: 68%. The Ne I photoelectron spectrum of Mo_2(*p*-CH_3-form)$_4$, however, does support the assignments of the valence ionizations. In a Ne I spectrum, the N- and C-based ionizations should increase in intensity by 16% and 36%, respectively, while those that are Mo-based ionizations should decrease by 11%.[35] As presented in Table 2, the intensities of the a_{1u} and e_g ligand-based ionizations increase markedly as compared to the Mo−Mo δ band.

Calculation of Valence Ionization Energies for Mo_2(form)$_4$ and W_2(form)$_4$. The ADF package readily allows the computation of valence ionization energies through the determination of the total energies of the neutral ground-state molecule and the various cationic species. Such a method provides a computational means of modeling the photoionization process by allowing the electronic structure to relax upon removal of an electron and is preferable to the use of molecular orbital energies from the ground-state calculation (i.e., Koopmans' approximation) to assign the photoelectron spectrum.

Calculated IPs for the Mo_2(form)$_4$ and M_2(HN(CH)NH)$_4$ (i.e., the original system with phenyl rings replaced by H atoms) at the Xα level are presented in Table 5. The most obvious difference between the two systems is that the four ligand-based ionizations are placed too low in energy when the phenyl rings are used in the calculation. In fact, these calculations predict that the lowest energy ionization results from the ligand a_{1u}

(35) Yeh, J. J.; Lindau, I. *At. Data Nucl. Data Tables* **1985**, *32*, 1−155.

Table 6. Valence Ionization Energies (in eV) Calculated with the ADF Package for $Mo_2(HN(CH)NH)_4$ Using the Xα and BLYP Methods in Comparison to the Experimental Values[a]

ionization	Xα	BLYP	exptl
Mo−Mo δ bond	5.23	5.70	5.63
ligand-based a_{1u}	5.59	6.13	6.45
ligand-based e_g	6.09	6.63	6.80
Mo−Mo π bond	6.97	7.51	7.32
Mo−Mo σ bond	7.15	7.67	
ligand-based b_{1u}	7.39	7.89	7.88

[a] Triple-ζ functions have been used on all atoms. Scalar relativistic corrections were employed.

Table 7. Valence Ionization Energies (in eV) Calculated with the ADF Package for $W_2(HN(CH)NH)_4$ Using the Xα and BLYP Methods in Comparison to the Experimental Values[a]

ionization	Xα	BLYP	exptl
W−W δ bond	4.77	5.21	5.23
ligand-based a_{1u}	5.70	6.25	6.58
ligand-based e_g	6.27	6.81	6.91
W−W π bond	6.42	6.93	7.33
W−W σ bond	7.49	8.01	7.54
ligand-based b_{1u}	7.68	8.17	7.91

[a] Triple-ζ functions have been used on all atoms. Scalar relativistic corrections were employed.

orbital, rather than from the Mo−Mo δ MO. Rotating the phenyl groups by 45°, as is observed in the crystal structure of Mo_2-(p-CH_3-form)$_4$, provides improved calculated ionization energies, but the N-based ionizations are still predicted to be slightly too low compared to those that are metal based. Rotating the phenyl groups so that they are perpendicular to the N−C−N plane gives the best relative ordering of the ligand- and metal-based valence ionizations, but the ionization from the ligand a_{1u} orbital is still calculated as being the easiest by about 0.1 eV. The most notable difference among these calculations in which the phenyl groups are rotated is the amount of N character in the ligand-based orbitals. With a planar ligand set, the ligand-based a_{1u} molecular orbital is composed of 53% N $p_\perp$ character. Rotating the phenyl groups by 45° increases the amount of N orbital character to 65% and although the first ionization is predicted to come from the a_{1u} orbital, the separation between this IP and that of the Mo−Mo δ bond decreases. This trend in increasing N character upon rotation of the phenyl groups and stabilization of the a_{1u} ionization relative to the δ ionization continues as the rings are rotated farther from the N−C−N plane. At this orientation, the a_{1u} orbital contains 91% N $p_\perp$ character. Only for this calculation is the ionization from the ligand-based e_g orbital predicted to be more difficult than that from the Mo−Mo δ bond.

Replacing the phenyl rings with H atoms, aside from increasing the speed of the calculation, provides reasonable ionization energies. For this abbreviated system, the valence ionizations are calculated to be in the same order as they have been assigned based on comparison of spectral features among the series, although the accuracy of the calculated values is somewhat poor. More reasonable valence ionization energies for the Mo and W systems have been calculated using the BLYP method and are presented in Tables 6 and 7, respectively.

Spectral Features of $Cr_2(form)_4$. The only distinct ionization peaks of the $Cr_2(form)_4$ molecule are due to the phenyl rings and the a_{1u} and e_g N-based orbitals. In comparison, the He I spectrum of $Cr_2(O_2CCH_3)_4$ shows that the ionization of electrons from the metal-based valence orbitals appears as a single broad band near 9 eV. Extrapolating the shifts observed for the W_2 and Mo_2 ionizations from the acetate to the formamidinate molecules, the Cr-based ionizations for $Cr_2(form)_4$ should be roughly near 7−8 eV and are therefore presumably coincident with the a_{1u} and e_g set of ligand-based orbitals as well as with the onset of the phenyl ionizations.

Table 8. Valence Ionization Energies (in eV) Calculated with the ADF Package for $Cr_2(HN(CH)NH)_4$ Using the Xα and BLYP Methods[a]

ionization	Xα	BLYP	exptl
Cr−Cr δ bond	5.27	5.80	6.44
ligand-based a_{1u}	5.49	6.05	6.66
ligand-based e_g	6.12	6.67	6.87
Cr−Cr π bond	6.85	7.35	7.08
Cr−Cr σ bond	7.17	7.67	
ligand-based b_{1u}	7.54	8.05	∼7.9

[a] Triple-ζ functions have been used on all atoms.

The spectrum of $Cr_2(form)_4$ does exhibit an ionization band at 6.4 eV, which appears as a leading shoulder on the front band. The energy separation between this band and the Mo−Mo δ ionization feature is 0.81 eV, which compares well with the separation of 0.86 eV observed for the $M_2(mhp)_4$ (M = Cr, Mo; mhp = 2-hydroxy-6-methylpyridine) spectra.[36] The photoelectron spectrum of $Cr_2(mhp)_4$ is the only one for which a separate ionization feature has been observed for the δ bond in a Cr−Cr quadruple bond-containing system. This feature is seen for the mhp system because of the increased ligand character in the Cr−Cr δ bond that is possible with the more Lewis basic N-donor ligand as well as for additional symmetry-related reasons. With the N-donor formamidinate ligand set, it appears here that the Cr−Cr δ ionization may also be separated from the σ and π features, although the proximity of the ligand-based a_{1u} and e_g ionizations renders such an assignment tentative.

Computationally determined ionization potentials for $Cr_2(HN(CH)NH)_4$ are presented in Table 8. The Cr−Cr δ ionization is calculated to be well separated from the σ and π ionizations by ca. 1.8 eV. The other metal- and ligand-based ionizations are calculated reasonably well although it is difficult to make exact assignments given the large number of overlapping features in the spectrum of $Cr_2(form)_4$.

Identifying the Ligand b_{1u} Ionization. As mentioned previously, the presence of a broad band of phenyl ionizations at 8.50 eV hinders the assignment of the b_{1u} ionization. This ionization, as shown in Figure 4, is from the ligand-based metal−ligand bonding molecular orbital that contains M−M δ* character and is found below the M−M σ MO. The saturated ligand, *N*,*N*′-dicyclohexylformamidine, has recently been used to prepare several dimetal paddlewheel compounds,[37,38] and because it lacks phenyl substituents, this ligand is ideal for attempting to observe the b_{1u} ionization. Close-up He I spectra of $Mo_2(form)_4$ and $Mo_2(cyform)_4$ are presented in Figure 10. Four peaks are visible in the $Mo_2(cyform)_4$ spectrum in the energy region 6.00−8.25 eV and a single ionization feature is present at 5.33 eV. The lack of a broad phenyl-based feature rising at 8 eV is evident. As in the He I spectrum of $Mo_2(form)_4$, the Gaussian bands representing the ionizations at 6.51 and 6.84 eV have an area ratio of 1:2 (current fit is 1:1.7) and are assigned as the a_{1u} and e_g peaks. The σ and π ionization feature, like the δ ionization, has moved to lower ionization energy relative to the phenylformamidinate species, but this region is best fit with two Gaussian functions at 7.19 and 7.43 eV. Finally, the resolved

(36) Garner, C. D.; Hillier, I. H.; MacDowell, A. A.; Walton, I. B.; Guest, M. F. *J. Chem. Soc., Faraday Trans. 2* **1979**, *75*, 485−493.
(37) Hao, S.; Gambarotta, S.; Bensimon, C.; Edema, J. J. H. *Inorg. Chim. Acta* **1993**, *213*, 65−74.
(38) Hao, S.; Berno, P.; Minhas, R. K.; Gambarotta, S. *Inorg. Chim. Acta* **1996**, *244*, 37−49.

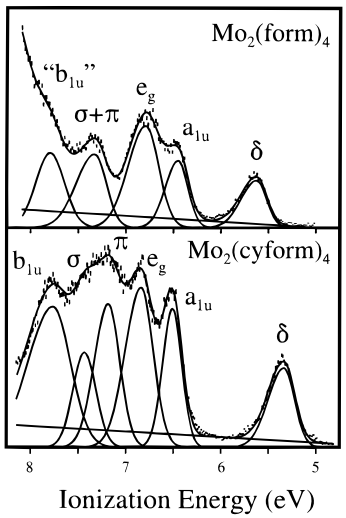

Figure 10. Detailed comparison of the lowest energy ionizations of $Mo_2(form)_4$ and $Mo_2(cyform)_4$.

band at 7.82 eV is the most likely candidate for the b_{1u} ionization. It appears at a similar energy position as the shoulder in the $Mo_2(form)_4$ spectrum.

It is interesting to note the similarity in energies of the ligand-based a_{1u}, e_g, and b_{1u} ionization features between the phenyl- and cyclohexyl-containing systems. Such a result suggests that the σ and π interactions between the phenyl and cyclohexyl rings and the N−C−N moiety are similar in these molecules. Further, it implies that the phenyl rings are not conjugated with the N−C−N π system in the gas phase, as they are not in the crystal structure of $Mo_2(form)_4$ where the phenyl rings are twisted from the plane of the N−C−N portion of the ligands. If the phenyl rings were coplanar with the N−C−N portion of the ligands, these ligand-based ionizations would be shifted about 1 eV to lower binding energies from those of the cyclohexyl-containing molecules. For example, such a shift is observed in the comparison of the first ionization of aniline with that of cyclohexylamine, where the filled−filled interaction between the N p_π orbital and a phenyl ring π orbital in aniline produces a low first ionization at 8.0 eV in comparison to the N lone pair ionization of cyclohexylamine at 9.1 eV. However, once this conjugation is lost, as occurs in $Mo_2(form)_4$, the inductive effects of the phenyl and cyclohexyl rings of the two ligands appear to be nearly equal as evidenced by the similarity in ionization energies of the ligand a_{1u}, e_g, and b_{1u} bands. The lack of conjugation with the phenyl rings is supported by the theoretical calculations discussed earlier, where the most accurate calculated ionization energies were obtained when the phenyl rings were twisted from the N−C−N plane, and the phenyl groups could be modeled reasonably with hydrogen atoms bound to the nitrogen atoms.

The difference in the shifts of the δ and π bands from $Mo_2(form)_4$ to $Mo_2(cyform)_4$ (0.30 vs 0.13 eV) emphasizes the different interactions that these metal-based orbitals have with the ligand. The δ bond interacts the most with the ligand. The shift of the metal−metal δ ionization may be due to a better overlap of the N $p_\perp$ orbital of cyform with the Mo−Mo δ bond or due to slight geometry changes between the two systems which require further investigation. The Mo−Mo σ bond can interact with the ligands in a σ fashion using the tori of the $4d_{z^2}$ AOs even though it is directed principally along the metal−metal bond axis rather than toward the ligand set. This ionization is the least sensitive to bonding interactions. The π bond has the appropriate symmetry to have an antibonding interaction with the N−C(H) bonds, but this combination is not expected to destabilize the metal−metal π bond nearly as much as is seen for the δ bond.

Conclusions

Comparisons between the photoelectron spectra of $M_2(form)_4$ (M = Cr, Mo, W) and those of the analogous $M_2(O_2CCH_3)_4$ compounds help to identify which ionizations are metal based and which are ligand based. For the systems $M_2(form)_4$ (M = Cr, Mo, W), ionizations attributed to the ligand-based a_{1u} and e_g MOs appear consistently at ca. 6.50 and 6.85 eV. The location of these two ionizations will assist the interpretation of the spectra of other $M_2(form)_4$ (M = Ru, Rh, Pd) systems. Although the fourth expected ligand ionization (b_{1u}) is obscured in the $M_2(form)_4$ systems, the He I photoelectron spectrum of $Mo_2(cyform)_4$ indicates the location of this ionization approximately 1 eV more stable than the a_{1u} and e_g ionizations. The σ, π, and δ predominantly metal-based ionizations can be assigned based on other trends between these homologous $M_2(form)_4$ systems. The relative energies of these ionizations are consistent with the better electron-donor ability of the formamidinates over the carboxylate ligands: the σ, π, and δ bands all appear at significantly lower ionization energies in the photoelectron spectra for these nitrogen-containing ligands than for the acetate systems. The changes in the energetic separations of the individual metal ionizations for a given compound are consistent with the symmetry properties and electron-donor properties of the formamidinates and carboxylates. The cyform ligand destabilizes the Mo−Mo δ ionization by 0.30 eV and appears to separate the Mo−Mo σ and π ionizations, thus assisting the assignment of the spectra of all of the compounds presented here.

As with the carboxylate systems, the He I photoelectron spectrum of $Cr_2(form)_4$ exhibits a single broad ionization band unlike the distinct ionization features that are observed in the photoelectron spectra of the analogous Mo_2 and W_2 compounds. The shoulder at ca. 6.4 eV appears to indicate that the Cr−Cr δ ionization is separate from the σ and π ionizations, analogous to that observed for $Cr_2(mhp)_4$. Such an observation supports the notion that the M−M δ bonds for the $M_2(form)_4$ (M = Cr, Mo, W) systems possess more ligand character than do the same orbitals for the dimetal tetraacetates.

Ultimately, these observations show greater metal−ligand mixing in the $M_2(form)_4$ systems than in the tetracarboxylates. The approximately 1 eV stabilization of the predominantly ligand b_{1u} ionization from the ligand a_{1u} and e_g ionizations represents a significant amount of bonding from ligand donation into the metal−metal δ^* orbital. Also, the ligand b_{2g} and b_{2g}^* orbitals and the metal−metal δ orbital comprise a three orbital/four electron set that is net bonding. The most stable combination is mostly ligand b_{2g} in character and is bonding between the metal and the ligands. The middle combination is mostly metal−metal δ in character and nonbonding with the ligands because the node is near the nitrogen atoms. The highest combination is antibonding between the metal and the ligands as well as antibonding within the ligands and is not occupied. The occupation of the metal−ligand bonding and nonbonding combinations results in a net bonding interaction. The ionization energy shifts show this interaction increasing from the tetraacetates to the tetraformamidinates and from Mo_2 to W_2. The closer energy proximity of the ligand-based a_{1u}, e_g, and b_{1u} ionizations to those from the metal-based σ, π, and δ bonds in $M_2(form)_4$ than in $M_2(O_2CCH_3)_4$ indicate the better energy match between ligand and metal fragment orbitals in the formamidinate systems required for the increased degree of covalency.

Acknowledgment. D.L.L. acknowledges support by the National Science Foundation (Grant No. CHE9618900) for studies of metal−metal bonding, the U.S. Department of Energy (Division of Chemical Sciences, Office of Basic Energy Science, Office of Energy Research, DE-FG03-95ER14574), and the Materials Characterization Program, Department of Chemistry, University of Arizona. M.H.C. also acknowledges support by the National Science Foundation (Grant No. CHE9405134). M.A.L. thanks the National Science Foundation for a predoctoral fellowship, Dr. Nadine Gruhn at the University of Arizona for helpful discussions, Prof. Sandro Gambarotta at the University of Ottawa for advice regarding the synthesis of the cyclohexylformamidine ligand, and Aaron Riechers for recollecting the spectrum of $Mo_2(O_2CCH_3)_4$ to confirm the energy of the Mo−Mo δ ionization.

JA993065E